Chinese Journal of
POLYMER SCIENCE

ARTICLE

https://doi.org/10.1007/s10118-021-2595-y
Chinese J. Polym. Sci. **2021**, *39*, 1459–1469

Tuning the Johari-Goldstein β-Relaxation and Its Separation from α-Relaxation of Poly(*n*-alkyl methacrylate)s by Small Molecule-bridged Hydrogen Bonds

Yuan-Biao Liu, Gao-Peng Shi, and Guo-Zhang Wu*

Shanghai Key Laboratory of Advanced Polymeric Materials, School of Materials Science & Engineering, East China University of Science & Technology, Shanghai 200237, China

Electronic Supplementary Information

Abstract Introducing small molecule-bridged hydrogen bonds (HBs) between polymer chains has been reported to effectively reduce the inter-chain cooperativity despite of strengthening the intermolecular interaction. Here, a systematic investigation on tuning the Johari-Goldstein β (β_{JG}) relaxation by adding various low-molecular-weight phenols in poly(*n*-alkyl methacrylate)s is carried out to further clarify the anomalous dynamics. Given these small molecules capable of coupling the motion with pendent groups of host polymers due to forming at least two HBs per molecule, poly(*n*-alkyl methacrylate) mixtures exhibit rich dynamic changes in the β_{JG}-properties and α, β_{JG} separations. An increased loading of phenols with a small size and strong inter-HB strength ($\Delta\upsilon_i$) clearly benefits for significant retardation and suppression of the β_{JG}-relaxation, narrows the α, β_{JG} separation and converges the β_{JG}-peak with the α-peak, which demonstrates the alleviation of inter-chain topological constraints. However, small molecules with a relatively big size and weak $\Delta\upsilon_i$ are found to amplify the magnitude of the α, β_{JG} separation of poly(butyl methacrylate), even though experimental results of changes in α-dispersion and dynamic fragility confirm a reduction of the coupling factor *n* in all of these hybrids. The counterintuitive phenomenon suggests that the crossover time t_c in the Coupling Model is no longer a universal quantity if the inter-chain interaction of polymers is strengthened by HBs. These compelling findings shed vital insights into the HB-induced anomalous dynamics, and provide essential guidance for tailoring the β_{JG} behavior and designing glassy polymeric materials.

Keywords Johari-Goldstein β-relaxation; Hydrogen bond; Glass transition; Poly(*n*-alkyl methacrylate); Small molecule

Citation: Liu, Y. B.; Shi, G. P.; Wu, G. Z. Tuning the Johari-Goldstein β-relaxation and its separation from α-relaxation of poly(*n*-alkyl methacrylate)s by small molecule-bridged hydrogen bonds. *Chinese J. Polym. Sci.* **2021**, *39*, 1459–1469.

INTRODUCTION

Polymers typically have a hierarchical structure with chainlike backbones and diverse branches or pendant groups; thus, they are ideal candidates for developing materials with high-performance and multi-functions. Among various secondary relaxations arising from the rotation or reorientation of pendant groups,[1,2] the Johari-Goldstein β (β_{JG}) process[3,4] is the slowest secondary relaxation chemically stemming from the flipping of side groups and the rocking of backbone. When temperatures drop to the vicinity of the glass transition temperature (T_g), the β_{JG}-relaxation decouples with the α-relaxation and remains active deep in the glassy state. Since the β_{JG}-relaxation may dominate many glassy polymer properties, such as gas permeability,[5−8] physical aging,[9] additive crystallization,[10−12] ductility and plastic deformation,[13] attempts to modify the β_{JG}-properties and manipulate its separation from α-relaxation have become an intense focus on developing advanced materials.

The β_{JG}-relaxation in physics originates from freely moving string-like units that have escaped from cooperativity within the frozen matrix, that is, a cascade of 'cage-breaking' events.[14] For simplified metallic glasses,[15−17] the β_{JG}-process seems to be determined by self-diffusion of the smallest metal atoms[18] and/or highly mobile atomic pairs.[19] Therefore, the β_{JG}-properties and its distance from α-relaxation have been tuned by incorporating different-sized atoms.[19] In glassy polymers having complex inter- and intramolecular interactions, the β_{JG}-process changes complicatedly with the motion of entire segmental units and their packing restrictions.[20−23] Polymers generally exhibit a weak and slow β_{JG}-relaxation when their pendent groups are enlarged either by covalent grafting with a bulky group[24,25] or by chemical substitution with a large atom.[26] However, once the incorporation of rigid component by means of crosslinking,[27,28] copolymerizing[29,30] and mixing[31−33] weakens the inter-chain packing efficiency, the β_{JG}-relaxation might be enhanced and accelerated to some extent.[27,30,32]

---

* Corresponding author, E-mail: wgz@ecust.edu.cn

Received February 7, 2021; Accepted April 20, 2021;

According to the Coupling Model proposed by Ngai,[34−36] the local β_{JG}-relaxation acts as a precursor of the cooperative α-relaxation, and the magnitude of the α, β_{JG} separation is a result of intermolecular constraints on cooperative α-relaxation as described:

$$\log\tau_{\alpha} - \log\tau_{JG} = n\left(\log\tau_{\alpha} + 11.7\right) \tag{1}$$

where τ_{JG} and τ_{α} are the relaxation time of β_{JG}- and α-relaxation, respectively, and coupling factor n captures the strength of topological constraints on α-relaxation.[34,36,37] Given that the dynamic heterogeneity of structural relaxation is a result of intermolecular constraint during segmental cooperative rearrangement, many experimental results confirmed that n = $1-\beta_{KWW}$, where β_{KWW} is the non-exponential stretching parameter described by the KWW equation,[38] *i.e.*, $\varphi(t) = \exp\left[-(t/\tau)^{\beta_{KWW}}\right]$. Therefore, a higher n or a lower β_{KWW} ($0<n$, $\beta_{KWW}\leq 1$) denotes a stronger deviation from pure exponential decay and broader α-dispersion in the frequency domain. Homopolymers with rigid backbone and bulky pendent groups typically have a high n and exhibit a large α, β_{JG} separation.[39−41] The magnitude of α, β_{JG} separation can be significantly altered by adding other components with different mobilities or T_g. In van der Waals-interacted copolymers,[29,30] miscible polymer blends,[31−33] and polymer/small molecule mixtures,[34,42] enhancing the intermolecular interaction either by crosslinking or by copolymerizing/mixing with a high-T_g component generally broadens the α-dispersion and increases the coupling factor n, thereby leading to a large α, β_{JG} separation.[34,43,44]

Polymer/small molecule hybrids driven by intermolecular hydrogen bonding (inter-HB) interactions have been studied and widely applied in many fields, including protein preservation,[45] drug release,[46] self-healing,[47] photoelectronic transportation,[48] and novel material preparation.[49−52] Tuning the β_{JG}-relaxation of polymers by the hydrogen-bonded small molecules will not only endow these hybrids with versatile and designable glassy properties to enrich their application prospects, but also help to understand the mechanism through which guest molecules induce the self-assembly and multi-functionality of host polymers. In contrast to van der Waals interactions and covalent bonds, small molecules with two or more functional groups act as physical crosslinkers and can form a transient hydrogen-bonding network among the polymer chains. This will substantially enhance the intermolecular interactions and result in a positive deviation of mixture's T_g from the linear additivity rule.[53,54] A logical conjecture is that introducing small molecule-bridged strong inter-HBs between polymer chains must strengthen the topological constraints, thereby broadening the α-dispersion and increasing the coupling factor n.

However, recent evidences apparently contradict the above conjecture. Runt *et al.*[55] firstly reported dynamic homogeneity of poly(vinyl methyl ether) by adding hydrogen-bonded small molecules. Our previous studies[56,57] further revealed that low-molecular-weight phenols capable of forming two hydrogen bonds per molecule can effectively narrow the α-dispersion (denoted as increased β_{KWW} or decreased n) of polyacrylates concomitant with a reduction of dynamic fragility even if the guest molecule has a T_g much higher than the host polymer. Given that the unavailability of free volume and topological constraint are the primary reason for segmental cooperative relaxation,[40] we suppose that introduction of small molecule-bridged hydrogen bonds not only alleviates the concentration fluctuation-induced broadening of α-dispersion,[58,59] but also reduces the inter-chain cooperativity despite of the HB-enhanced intermolecular interaction. The reduced inter-chain cooperativity was rationalized in terms of small molecule-alleviated long-chain connectivity, balanced flexibility of bulky pendant groups relative to backbones and enhanced enthalpic contributions to segmental cooperative rearrangement.[56] Accordingly, a systematic study on variation of the β_{JG}-relaxation by introducing small molecule-bridged hydrogen bonds shall further clarify the anomalous dynamics by identifying whether it shortens the α, β_{JG} separation and leads to encroachment of the β_{JG}-peak by the α-peak.

In this work, we mixed low-molecular-weight phenols with poly(methyl methacrylate) (PMMA) and poly(butyl methacrylate) (PBMA) to adjust the polymers' β_{JG}-processes. Inter-HB network throughout the matrix was found to act as a bridge capable of coupling the motion between guest molecules and pendent groups of the host polymers. By changing the size of hindered phenols and the inter-HB strength ($\Delta\upsilon_i$), we observed rich dynamic changes in β_{JG}-properties and α, β_{JG} separations of these poly(n-alkyl methacrylate)s, which are completely different from those in copolymers and miscible mixtures with van der Waals interactions. Interestingly, despite of effectively reducing inter-chain cooperativity/constraints due to the formation of small molecule-bridged inter-HB networks, a suppressed β_{JG}-peak with amplified magnitude of the α, β_{JG} separation was observed in systems with adding bulky small molecules.

EXPERIMENTAL

Materials

4,4′-Thio-bis(6-*tert*-butyl-*m*-methyl phenol) (AO300, T_g=302 K, n=0.43, dipole moment μ=2.5 D), 4,4′-thiodiphenol (TDP, T_g ~ 210 K, μ=3.0 D), 1,3,5-trimethyl-2,4,6-tris(3,5-di-*tert*-butyl-4-hydroxybenzyl) benzene (AO330, T_g=368 K, n=0.46, μ=1.8 D), and PMMA (M_w=90 kg/mol, PDI=1.90, T_g=381 K, μ=1.7 D) were provided by Aladdin. 1,1,3-Tris(2-methyl-4-hydroxy-5-*tert*-butylphenyl) butane (CA, T_g=371 K, n=0.53, μ=2.0 D) was provided by Tianjin Lisheng Chemical. PBMA (M_w=330 kg/mol, PDI=2.27, T_g=298 K, μ=1.8 D) was synthesized *via* solution polymerization under a nitrogen atmosphere by using azobis(isobutyronitrile) (AIBN, ≥99.5%, Aldrich) as an initiator. All reagent molecules were used as received, and their chemical structures are plotted in Fig. 1.

Sample Preparation

The polymer was dissolved in ethyl acetate (EAc) solution at a concentration of 20 wt% with continuous stirring. Small molecules were then added and stirred until completely dissolved to prepare hybrids with different additive weight concentrations. The solution was cast into the glass mold, kept at room temperature for 48 h, and further dried under vacuum at 120 °C for 2 h to ensure a complete evaporation of solvents.

Broad Band Dielectric Spectrometer (BDS)

The dielectric spectra were collected with a Novocontrol

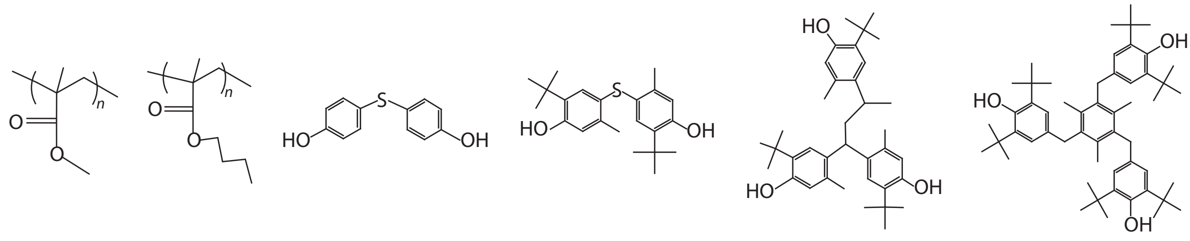

(a) PMMA (b) PBMA (c) TDP (d) AO300 (e) CA (f) AO330

Fig. 1 Molecular structures of (a) PMMA, (b) PBMA, (c) TDP, (d) AO300, (e) CA and (f) AO330.

Concept 40 broad band dielectric spectrometer in the frequency domain of 0.01 Hz to 10 MHz. Samples with a diameter of 20 mm and a thickness of 250 μm were prepared *via* hot pressing above the T_m of small molecules, followed by a quenching process. The temperatures were controlled within 0.1 K with a Novocontrol Quatro Cryosystem, and liquid N_2 was used to cool the samples. The dielectric loss spectra were fitted using a single or multiple Havriliak-Negami (HN) Eq. (2):[60,61]

$$\varepsilon^*(\omega)=\varepsilon_\infty+\sum_i \frac{\varepsilon_{0i}-\varepsilon_{\infty i}}{\left[1+(j\omega\tau_{\mathrm{HN}i})^{a_i}\right]^{b_i}}-j\left(\frac{\sigma}{e_0\omega}\right)^s \qquad (2)$$

where ε^* represents the complex dielectric permittivity. $\Delta\varepsilon=\varepsilon_0-\varepsilon_\infty$ is the dielectric strength, where ε_0 and ε_∞ are the relaxed and unrelaxed dielectric constants at extremely low and high frequencies, respectively. a_i and b_i ($0<a_i$, $b_i\leq 1$) are shape parameters of relaxation process i (primary or secondary) that represent symmetric and asymmetric broadening, respectively. σ is the ionic conductivity, e_0 (8.854 pF/m) is the free space dielectric permittivity, and s is a parameter very close to the unit.[60] τ_{HN} is the relaxation time by HN equation and is used to obtain the peak location $\tau_{\max}$:[62]

$$\tau_{\max}=\tau_{\mathrm{HN}}\left(\sin\frac{ab\pi}{2(b+1)}\right)^{1/a}\left(\sin\frac{a\pi}{2(b+1)}\right)^{-1/a} \qquad (3)$$

In the PBMA hybrids, we set $b<1$ for asymmetric primary α-peaks, and $b=1$ for symmetric secondary β_{JG}-peaks. The PMMA hybrids have an unusually asymmetric secondary β_{JG}-peak with $b<1$.[63,64] The HN fitting procedures for PBMA or PMMA mixtures are clearly shown in the Supporting Information (Figs. S1−S5, Tables S1 and S2 in the electronic supplementary information, ESI). The increase of temperature results in an accelerated β_{JG}-process (as manifested by a higher peak frequency) with enhanced peak intensity. The increase of temperature also accelerates α-process, but it reduces the intensity of α-process due to the weakening α-cooperativity.

RESULTS AND DISCUSSION

Effect of AO300 Concentration on the β_{JG}-Relaxation

Fig. 2(a) shows the dielectric loss ε'' near T_g of PMMA containing different amounts of AO300. It can be observed that neat PMMA displays a prominent and well-resolved β_{JG}-peak at the high-frequency flank of α-peak whose strength is nearly twice as that of α-relaxation as previous reports.[63,64] The addition of AO300 substantially enhances the α-peak intensity and simultaneously reduces the β_{JG}-intensity, thereby leading to a diminishing β_{JG}-peak that merges gradually with α-peak. HN fitting curves are given for better identifying the respective peak times. Fig. 2(a) also depicts the temperature dependence of the α- and β_{JG}-relaxation time for these PMMA/AO300 hybrids. We can see that the addition of AO300 accelerates α-relaxation of PMMA (decreased τ_α) at a given temperature. Meanwhile, the β_{JG}-motion of PMMA is apparently restricted, as manifested by an increased τ_{JG}, after hydroxyl groups of AO300 are hydrogen bonded to the carbonyl moiety of the PMMA side group as detected by FTIR analysis.[52] These results demonstrate that AO300 acts typically as an anti-plasticizer[65−67] in the PMMA matrix.

Neat PBMA exhibits a prominent β_{JG}-process whose intensity is close to that of the α-relaxation (Fig. 2b). Compared to rigid PMMA, the flexible PBMA exhibits a distinguishable β_{fast}-peak (the dependence of β_{fast}-peak time and intensity on temperature is shown in Fig. S2 in ESI) at a frequency near to 10^6 Hz, and a small α, β_{JG} separation due to the reduction in coupling factor n caused by the inner plasticizing effect of flexible butyl group.[39] Addition of AO300 results in the slowing down of both α- and β_{JG}-relaxations, as well as a narrowed α, β_{JG} separation. As will be further discussed below, we have confirmed that both the β_{fast}-peak and the suppressed β_{JG}-peak in Fig. 2(b) are resulted from the cooperative impact of the polymer chain and the small molecule, rather than from the extra relaxation modes of the additives. The addition of AO300 in PBMA leads to a weak and slow β_{JG}-relaxation as PMMA, clearly demonstrating that phenolic molecules act like the chemical modification of side group and effectively restrict the β_{JG}-relaxation of poly(n-alkyl methacrylate)s when they are hydrogen bonded to the carbonyl moiety of acrylic pendent groups.

Separation of the β_{JG}-peak from the α-peak of PBMA and PBMA/phenol mixtures is particularly difficult by HN fittings due to their overlapping near T_g. We recognize that the multiple HN fittings must create large uncertainties in determining the dispersion of α- and β_{JG}-peaks,[68] despite that the uncertainties of the most probable intensity and peak time can be effectively minimized if the HN fitting is carefully performed under procedures given in Fig. S1 (in ESI).[68,69] Therefore, the dashed fitting curves for the PBMA systems in this work are just for guide of eye to identify the position of various peaks. As shown in Fig. 2(a), with the acceleration of the α-relaxation and the slowing down of the diminishing β_{JG}-relaxation, the α- and β_{JG}-traces of the PMMA/AO300 hybrids gradually move closer to each other, and the β_{JG}-peak cannot be resolved from the α-peak when the AO300 content reaches 75 wt% (Fig. S6 in ESI). The PBMA/AO300 hybrids also display a reduced α, β_{JG} separation (Fig. 2b and Table 1) due to the fact that AO300 molecules more significantly slow down the β_{JG}-relaxation than the α-relaxation. Notably, when

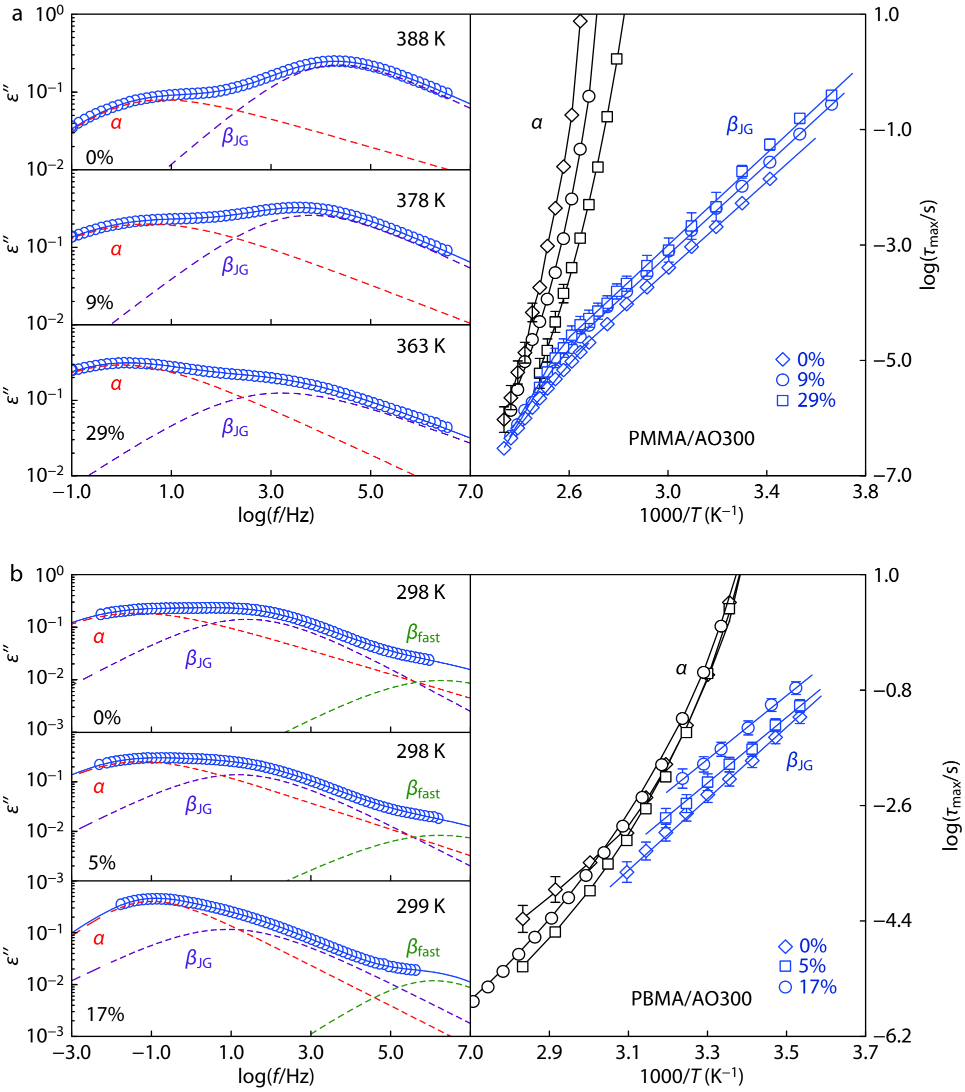

Fig. 2 Dielectric loss ε″ at indicated temperatures near T_g and temperature dependence of the α- and β_{JG}-relaxation time for (a) PMMA and (b) PBMA hybrids containing different AO300 loadings. The dashed red, purple and green curves represent the HN fittings of α-, β_{JG}- and β_{fast}-peaks, respectively.

the loading of AO300 exceeded 17 wt%, β_{JG}-relaxation of PBMA is encroached by α-relaxation and cannot be resolved well from α-relaxation. At 50 wt%, β_{JG}-relaxation is suppressed completely (Fig. S7 in ESI).

Effect of Molecule Size on the β_{JG}-Relaxation

The triphenyl-ring CA (V_w=373 cm^3/mol) molecule has a similar steric hindrance as AO300 (V_w=229 cm^3/mol) on hydroxyl groups (Fig. 1); thus, despite of bulkier van der Waals volume (V_w) and capability of forming triple inter-HBs per molecule, it owns an inter-HB strength $\Delta\upsilon_i$ (158 cm^{-1}, determined by FTIR analysis as shown in Figs. S8 and S9 in ESI) very close to AO300 ($\Delta\upsilon_i$=167 cm^{-1}) at ambient temperatures. Fig. 3(a) shows dielectric loss ε″ curves and temperature dependence of the α- and β_{JG}-relaxation time for PMMA containing 0 wt%, 17 wt% and 60 wt% CA. The addition of CA substantially enhances the α-intensity and simultaneously reduces the β_{JG}-intensity, which is in similar tendency as AO300-loaded PMMA mixtures. However, different from the AO300 system, the CA molecule with a comparable T_g to that of PMMA matrix trivially affects the τ_α of PMMA. Furthermore, an unrestricted β_{JG}-motion, as manifested by little change in τ_{JG}, can be observed when bulkier CA molecules are added. We observe a slight acceleration of τ_{JG} with increasing CA loading (Fig. 3a), a trend which is different from the τ_{JG} change in the case of adding AO300.

When the bulky CA mixes with the flexible PBMA matrix, a remarkable increase in τ_{JG} (Fig. 3b) is observed, suggesting a substantially constrained β_{JG}-motion of PBMA. Addition of 17 wt% CA leads to an increase in β_{JG}-peak temperatures at τ_{max}=1 s (T_{JG}) of PBMA about 9 K (Table 1), which is higher than the increment in T_{JG} (6 K) of the PBMA/AO300 hybrids at the same content range. Due to the large mobility difference between CA and PBMA, bulky CA molecules more significantly slow down the α-relaxation than the β_{JG}-relaxation of PBMA (Fig. 3b). Consequently, the α- and β_{JG}-traces of the PBMA/CA hybrids separate from each other with increasing CA content. We noticed again a decrease in τ_{JG} of the

Table 1 Inter-HB strength at T_α ($\Delta\upsilon_i$), van der Waals volume of hindered phenols (V_w), β_{JG}-activation energy (E_{JG}, at $T<T_g$), α- and β_{JG}-peak temperature at τ_{max}=1 s (T_α, T_{JG}), width of α- and β_{JG}-peak (T_α–T_{JG}), fragility *m* (at τ_{max} =1 s) of PMMA and PBMA mixed with different amounts of various hindered phenols.

Sample	Concentration (wt%)	$\Delta\upsilon_i$ at T_α (cm^{-1})	V_w (cm^3/mol)	E_{JG} (kJ/mol)	T_{JG} (K)	T_α (K)	T_α–T_{JG} (K)	*m*
PMMA/AO300	0%	/	229	73	256	381	125	107
	9%	154		72	262	371	109	91
	17%	155		68	264	365	101	87
	29%	156		66	267	359	92	77
	75%	161		/	/	328	/	67
PMMA/CA	17%	144	373	70	254	374	120	98
	60%	144		69	249	373	124	73
PBMA/AO300	0%	/	229	98	267	298	31	62
	5%	167		90	268	298	30	56
	9%	167		84	272	300	28	53
	17%	167		82	273	301	28	48
	29%	166		/	/	302	/	48
	50%	165		/	/	307	/	54
PBMA/TDP	17%	313	113	78	274	280	6	40
PBMA/CA	9%	155	373	90	269	315	46	48
	17%	153		79	275	323	48	50
	29%	151		77	278	334	56	53
	60%	147		72	264	351	87	66
PBMA/AO330	9%	103	515	90	267	302	35	55
	17%	102		84	267	312	45	56
	50%	101		83	261	335	74	71

Note: "/" denotes data not detectable.

PBMA/CA hybrids as the CA loading reaches 60 wt%. This phenomenon arises from a weakened $\Delta\upsilon_i$ at the increased T_g, which will be further discussed in the next section.

Effect of Inter-HB Strength on the β_{JG}-Relaxation

A robust inter-HB is crucial for coupling the motion between the guest molecules and the acrylic pendent groups. To elucidate the effect of the inter-HB strength $\Delta\upsilon_i$ on the β_{JG}-properties, various phenolic molecules with adjusted van der Waals volume (V_w) and steric hindrance on their hydroxyls were mixed with the PBMA matrix. Among them, AO330 (V_w=515 cm^3/mol, $\Delta\upsilon_i$=103 cm^{-1}) has a larger bulkiness but a weaker $\Delta\upsilon_i$ than CA (V_w=373 cm^3/mol, $\Delta\upsilon_i$=158 cm^{-1}), whereas TDP (V_w=113 cm^3/mol, $\Delta\upsilon_i$=313 cm^{-1}) has a smaller size but a stronger $\Delta\upsilon_i$ than AO300 (V_w=229 cm^3/mol, $\Delta\upsilon_i$=167 cm^{-1}). Note that the $\Delta\upsilon_i$ mentioned here is determined at ambient temperatures, while in Table 1 it is at T_g.

Compared to the β_{JG}-traces of PBMA with adding CA, Fig. 4 shows that adding bulky AO330 with a weak $\Delta\upsilon_i$ has little effect on change in τ_{JG} of PBMA, though intensity of the β_{JG}-peak is suppressed remarkably. By contrast, the rigid AO330 significantly restricts the segmental relaxation of PBMA, thereby leading to an apparent increase in τ_α or T_α of the PBMA/AO330 hybrids. As a result, the α- and β_{JG}-traces of the PBMA/AO330 hybrids gradually separated from each other with increasing AO330 content, and the significant increase in τ_α or T_α is responsible for the increased α, β_{JG} separations. On the contrary, addition of small TDP molecules with a stronger $\Delta\upsilon_i$ effectively restricts the β_{JG}-motion of PBMA and leads to a remarkable increase in τ_{JG} of PBMA as shown in Figs. S10 and S11 (in ESI). Compared with the β_{JG}-traces in PBMA/AO300 hybrids, the β_{JG}-peak of PBMA rapidly converges with α-peak after adding TDP, and the β_{JG}-peak becomes un-resolvable when TDP loading exceeds 17 wt%. We noted that the TDP mixtures exhibit more pronounced α-, β_{JG}- and β_{fast}-peaks than AO300, CA and AO330 mixtures (Fig. S11 in ESI). This may be rationalized by the fact that TDP (μ=3.0 D) has the largest dipole moment among these additives. However, variations of intensity, relaxation time and activation energy of the secondary relaxations with the TDP loading exhibit a similar tendency as that of AO300 mixtures (Fig. 5 and Fig. S12 in ESI), further verifying that the β_{JG}-peak stems from the hydrogen bonding-induced cooperative impact of PBMA and TDP, rather than from the independent relaxation of TDP.

Fig. 5 shows a comparison of τ_{JG} at different temperatures for PBMA hybrids containing different types of small molecules. The loading is given at 17 wt%. As is seen, the temperature dependence of τ_{JG} in all PBMA hybrids follows Arrhenius fashion with slightly varied activation energies from 77 kJ/mol to 84 kJ/mol. At a given temperature (for example, at 280 K denoted by the dashed arrow in Fig. 5), the τ_{JG} is found to increase with increasing $\Delta\upsilon_i$ in the order AO330<AO300<TDP. Clearly, a stronger $\Delta\upsilon_i$ between the small molecule and the polymer chain leads to a more restricted β_{JG}-motion and a longer τ_{JG}. Apart from the significant effect of $\Delta\upsilon_i$, we also note a longer τ_{JG} in the CA mixture than that in the AO300 system, and the τ_{JG} in the CA mixture is slightly longer than that in the high-$\Delta\upsilon_i$ TDP mixture. These results highlight a strong impact of the additive size and demonstrate that a bulkier molecule is also beneficial for a more restricted β_{JG}-motion.

Generally, $\Delta\upsilon_i$ decreases with increasing temperatures and its temperature dependence shall change a little with the type of small molecules (Figs. S8 and S9 in ESI). These variations may provoke slight changes in the activation energy (E_{JG}) of τ_{JG}. We observe in Fig. 4 that the τ_{JG} of the PBMA/AO330 at high-temperature range is longer than that

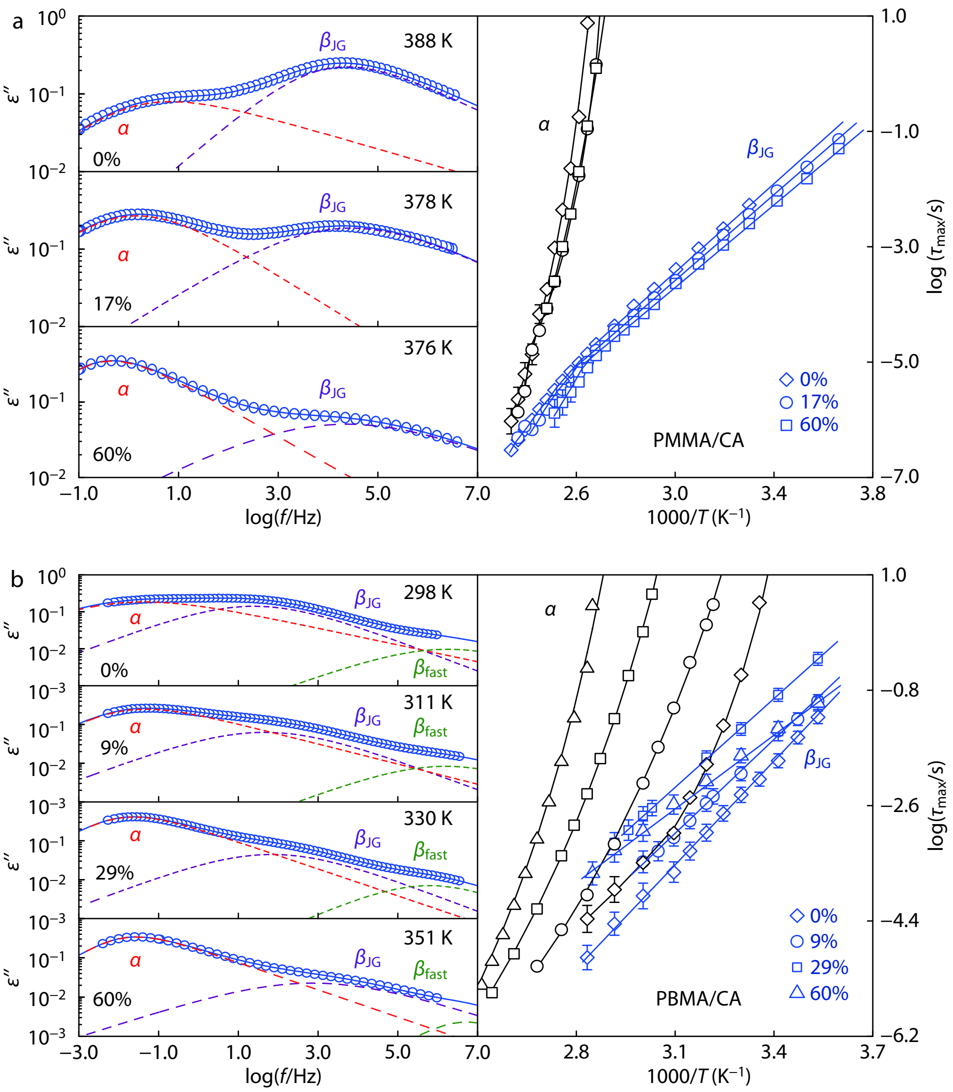

Fig. 3 Dielectric loss ε'' at indicated temperatures near T_g and temperature dependence of the α- and β_{JG}-relaxation time for (a) PMMA and (b) PBMA hybrids containing different amounts of CA (wt%). The dashed red, purple and green curves represent the HN fittings of α-, β_{JG}- and β_{fast}-peaks, respectively.

of neat PBMA whereas at low-temperature range it becomes shorter. The variation of $\Delta\upsilon_i$ with temperatures can also account for the decrease of τ_{JG} in PBMA/CA hybrids when a high CA content is loaded (Fig. 3b): at a loading of 60% CA, T_g of PBMA increases significantly from 298 K to 351 K, leading to the apparent reduction of $\Delta\upsilon_i$ from 158 cm^{-1} to 147 cm^{-1} (Table 1). If the PBMA matrix is replaced by high-T_g PMMA, a reduction of $\Delta\upsilon_i$ can also be observed near the T_g of the mixtures (Table 1 lists T_g and the corresponding $\Delta\upsilon_i$ for various mixtures). This fact can explain why its τ_{JG} decreases slightly with increasing CA loadings (Fig. 3a).

Effect of Small Molecule-bridged HBs on α, β_{JG} Separation

Fig. 6(a) depicts the effect of small molecule loading on the α, β_{JG} separation, which is denoted by the time span $\log\tau_\alpha - \log\tau_{JG}$ at τ_α=10 s. As seen, the $\log\tau_\alpha - \log\tau_{JG}$ of PMMA is apparently reduced with the addition of AO300, while it decreases slightly by adding bulky CA. The α- and β_{JG}-peaks of PBMA converge when TDP and AO300 are added. According to Eq. (1), the decreased $\log\tau_\alpha - \log\tau_{JG}$ strongly demonstrates the fact that the inter-chain cooperativity/constraints must be reduced, that is, a decreased coupling factor n by introducing small molecule-bridged inter-HBs despite of the HB-strengthened intermolecular interactions.

However, we observed a gradual separation between α- and β_{JG}-peaks of PBMA with increasing loadings of CA and AO330, a trend completely different from other systems shown in Fig. 6(a). Furthermore, we found an enlarged separation with the increasing bulkiness of small molecules. Fig. 6(b) shows the normalized size ($V_w/V_{w(BMA)}$) dependence of the α, β_{JG} separation in PBMA hybrids at a given loading of 17 wt%. Clearly, the $\log\tau_\alpha - \log\tau_{JG}$ monotonically increases with the V_w of hindered phenols. At first glance, this trend appears reasonable because the attachment of bulky phenolic molecules to acrylic ester groups *via* inter-HBs can be regarded as enlarging the acrylic pendent groups and may im-

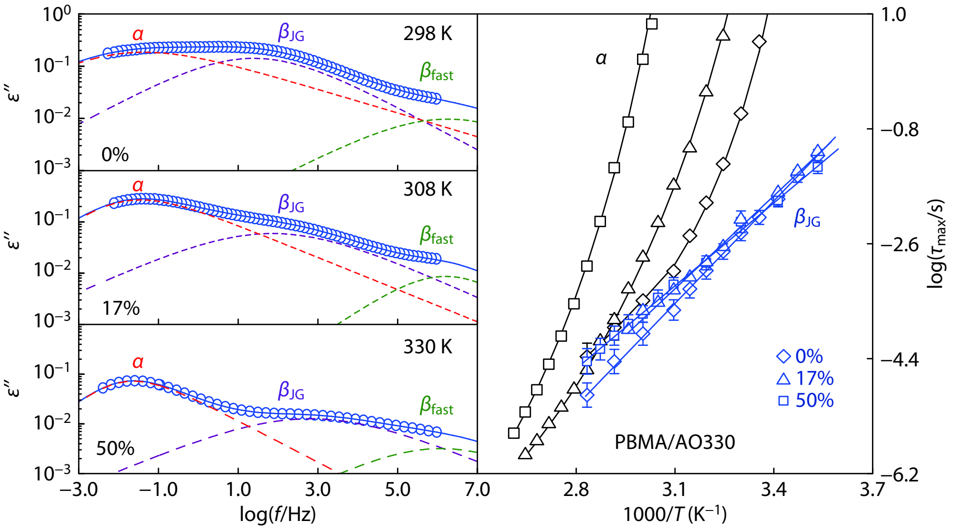

Fig. 4 Dielectric loss ε″ at indicated temperatures near T_g and temperature dependence of α- and β_{JG}-relaxation time for PBMA hybrids containing 0 wt%, 17 wt%, and 50 wt% AO330. The dashed red, purple and green curves represent the HN fittings of α-, β_{JG}- and β_{fast}-peaks, respectively.

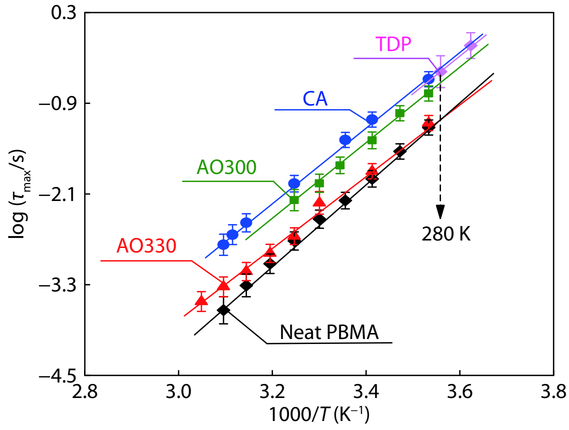

Fig. 5 Temperature dependence of β_{JG}-relaxation time for PBMA hybrids mixed with different phenols at a given loading of 17 wt%.

pose greater steric hindrance effects on the segmental relaxation of flexible PBMA. However, if this was true, then addition of CA and AO330 in PBMA should strengthen topological constraints on segmental cooperative rearrangement during glass transition and leads to an increased coupling factor *n*.

To elucidate the changes in topological constraints, we checked the effect of CA and AO330 loadings on the α-dispersion of PBMA because a broad α-dispersion corresponds to an increased *n*. Due to the uncertainties of α-dispersion by HN fittings in poly(*n*-alkyl methacrylates),[68] the normalized α-dispersion curves are explored in the following analysis. As shown in Figs. 7(a) and 7(b), the narrowing trend in α-dispersion of PBMA/CA and PBMA/AO330 hybrids is distinguishable with increasing small molecule loadings, though it is interfered by the β_{JG}-peak at the high-frequency flank of α-peak. When the loading exceeds 17 wt%, the narrowing effect becomes clearer as the β_{JG}-peak is dramatically sup-

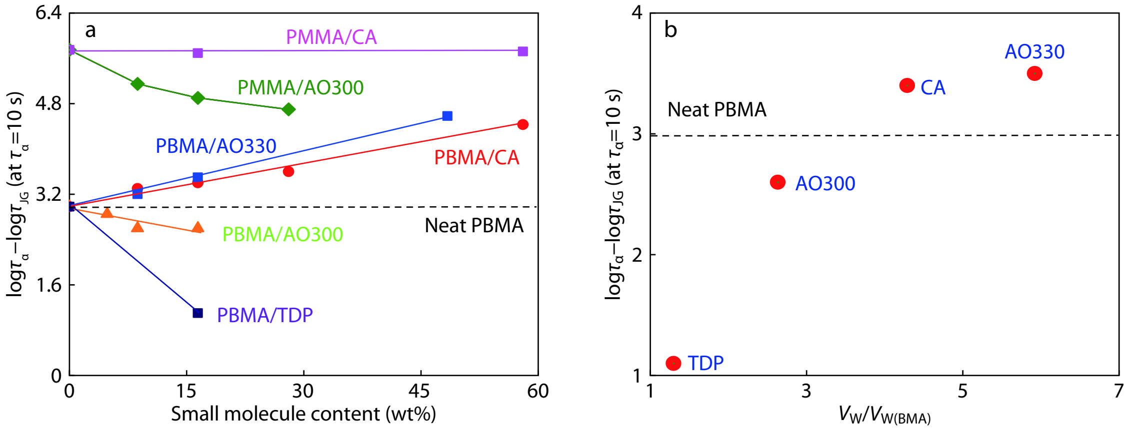

Fig. 6 (a) Effect of small molecule loading on α, β_{JG} separation (logτ_α−logτ_{JG}) at τ_α=10 s for PMMA and PBMA mixed with various hindered phenols. (b) Effect of small molecule size (V_w) on logτ_α−logτ_{JG} at τ_α=10 s for PBMA hybrids containing different phenols at a loading of 17 wt%. Here, the van der Waals volume (V_w) of small molecules is normalized by the V_w of PBMA monomer unit ($V_{w(BMA)}$=87 cm^3/mol).

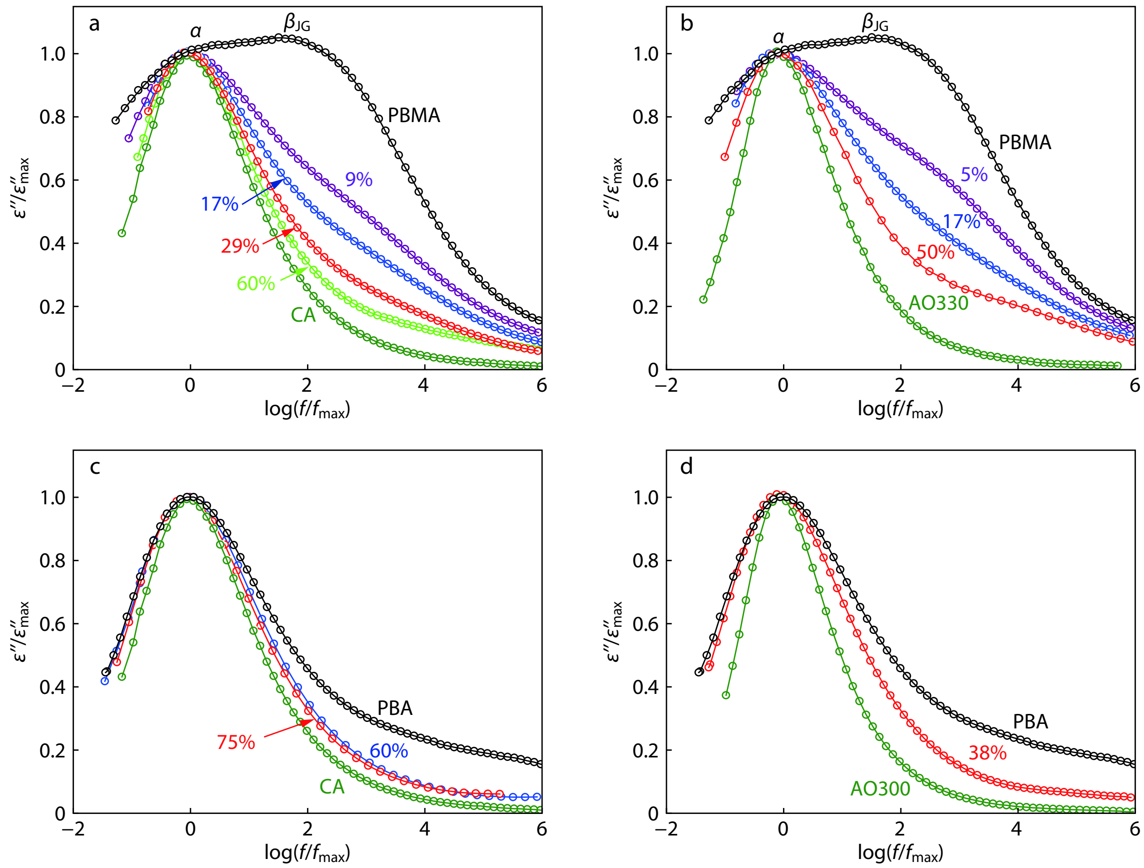

Fig. 7 Normalized α-loss spectra near T_g of (a) PBMA/CA, (b) PBMA/AO330, (c) PBA/CA and (d) PBA/AO300 hybrids containing different amounts of small molecules.

pressed and becomes resolvable from the giant α-peak. To remove the influence from the β_{JG}-peak, we change the matrix to be poly(butyl acrylate) (PBA), a homologue of PBMA with a much lower T_g and independent α-loss peaks. Although PBA has a T_g that is, respectively, 74 and 137 K lower than AO300 and CA, both of PBA/CA and PBA/AO300 mixtures exhibit a definitely narrowing α-dispersion (Figs. 7c and 7d) with increasing additive content, demonstrating the promoted dynamic homogeneity or reduced inter-chain constraints of PBA by adding CA and AO300.

Dynamic fragility m quantifies the variation steepness of τ_α with T_g-scaled temperature at $T=T_g$.[70] It measures how cooperative the α-relaxation is, and a decrease in m is generally a consequence of reduced α-cooperativity.[36,37] As shown in Fig. 8, although a higher $\Delta\upsilon_i$ can more positively promote T_g (AO330<CA<AO300), the HB-driven hybrids exhibit an apparently lower m than both of its two constituting components at additive contents lower than 29 wt%, and a stronger $\Delta\upsilon_i$ between phenolic hydroxyl and acrylic carbonyl groups leads to a more substantial decrease in m. Accordingly, the inter-chain constraints must be alleviated by small molecule-bridged inter-HB networks, further supporting that the coupling factor n of PBMA is reduced by adding CA and AO330.

Universality of Crossover Time t_c

The question is why the α, β_{JG} separations increase with decreasing coupling factor n for CA and AO330-loaded PBMA hybrids. It is essential to re-identify whether the sub-T_g secondary process is the β_{JG}-relaxation as it may be encroached by other relaxation modes of small molecules or stem from the α-relaxation due to phase separation of small molecules. In the present work, the narrowing dielectric α-dispersion (Fig. 7) together with an independent heat capacity (C_p) jump in differential scanning calorimetry (DSC) (Fig. S15 in ESI) confirm that small molecules are uniformly dispersed in polyacrylate matrix. Moreover, the continuous changes in dielectric spectra (Fig. S13 in ESI) of PBMA hybrids with increasing temperature or small molecule content can also exclude the untenable conjectures. We confirmed that small molecules used in this study display no β_{JG}-relaxations (Fig. S13d in ESI) and their β_{fast}-relaxations are well separated from the β_{JG}-relaxations of PBMA (Fig. S14 in ESI). Furthermore, phase separation gives rise to α-relaxation time obeying the VFT fashion, which is in contrary to the Arrhenius type found in all secondary traces of PBMA hybrids. More importantly, if phase separation took place, an enhancement in peak intensity should be observed with the increasing small molecule's loading. The suppressed β_{JG}-peak observed in the present work clarifies that it must not be the extra relaxation mode of additives phase separated from the polymer matrix. In addition, the activation energy of the secondary process (E_{JG}, listed in Table 1) calculated from the Arrhenius plots of relaxation time approaches to the prediction by $E_{JG}=26RT_g$[71] as the loading of small molecules increases to be higher than 17 wt% (the predicted E_{JG} is in a range of 65–

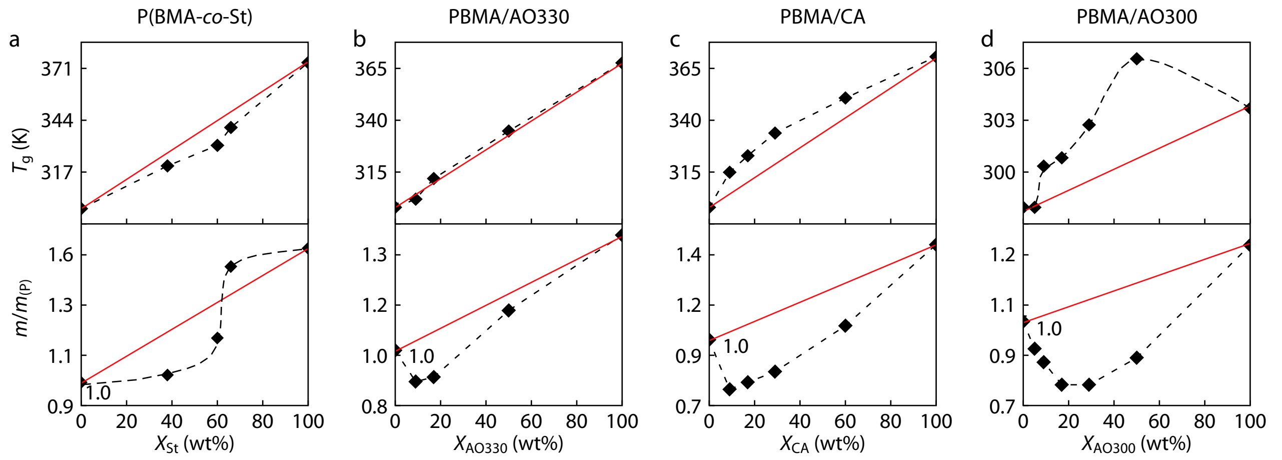

Fig. 8 Concentration dependence of T_g, $m/m_{(P)}$ of (a) P(BMA-*co*-St), (b) PBMA/AO330, (c) PBMA/CA, and (d) PBMA/AO300. T_g and m were determined at τ_{max}=1 s, and m is normalized by the neat PBMA's own m ($m_{(P)}$). For comparison, concentration dependence of T_g, $m/m_{(P)}$ of the P(BMA-*co*-St) is given in (a) based on data from work of Kahle *et al.*[30] Here, P(BMA-*co*-St) is a copolymer of butyl methacrylate (BMA) and styrene (St).

76 kJ/mol). All of these evidences assert that the secondary peaks around the α-peak flank must originate from the β_{JG}-relaxation of PBMA that is restricted by bulky phenols *via* inter-HB interactions, rather than from the extra relaxation modes of additives.

The Coupling Model proposed by Ngai provides a connection between the cooperative τ_α and primitive τ_{JG} *via* coupling factor n through the following Eq. (4):

$$\log\tau_\alpha - \log\tau_{JG} = n\left(\log\tau_\alpha - \log t_c\right) \qquad (4)$$

where t_c is time at the crossover from exponential to non-exponential decay, the magnitude of which is entirely determined by the interaction potential. Given that t_c = 2 ps, Eq. (4) can be simplified to Eq. (1). The prediction of the α, β_{JG} separations by Eq. (4) works well for weakly-interacted carbon-based small molecular/ionic glass-formers and polymers, because crossover time t_c in these systems keeps nearly constant at about 1−2 ps and is insensitive to temperature or pressure.[72]

The counterintuitive phenomenon that separation of the β_{JG}-peak from the α-peak by reducing n in this study can be rationalized only when one assumes that the crossover time t_c is not a universal quantity and decreases with increasing $\Delta\upsilon_i$. For example, the $\log\tau_\alpha$–$\log\tau_{JG}$ of PBMA is 2.98 (see Fig. 6a), which corresponds to a value of n=0.23 according to Eq. (1). If the addition of 17 wt% TDP or AO300 leads to a reduction of n from 0.23 to 0.18 (the same decrement of n in PEA/TDP hybrids as previously reported)[56] and a decrease in t_c from 2 ps to 0.02 ps, then $\log\tau_\alpha$–$\log\tau_{JG}$ decreases from 2.98 to 2.65 as expected. Since adding bulky molecules like CA and AO330 must alleviate the reduction of n, given that n=0.22 and t_c=0.02 ps, then $\log\tau_\alpha$-$\log\tau_{JG}$ increases to 3.23. That is to say, if t_c minimizes by introducing small molecule-bridged HBs between polymer chains, one can observe the anomalous dynamics that the β_{JG}-peak separates from the α-peak despite of reducing its inter-chain cooperativity.

Actually, t_c decreases with increasing $\Delta\upsilon_i$, which has been verified by molecular dynamics simulations of imidazolium-based ionic liquids.[73] In that case, the formation of HB interactions engenders severe anharmonic chaos on the rotation motion of ions, which significantly reduces the t_c value by nearly 2 orders of magnitude (from 1 ps to ~0.02 ps).

CONCLUSIONS

The β_{JG}-relaxation of poly(n-alkyl methacrylate)s and its separation from α-relaxation could be effectively tuned by introducing hindered phenol-bridged HBs. The β_{JG}-relaxation can be effectively suppressed and retarded when bulky hindered phenols are attached to the acrylic pendent groups *via* a strong $\Delta\upsilon_i$, while it is trivially affected or even accelerated in case of weak $\Delta\upsilon_i$ or rigid polyacrylate matrix (like PMMA). The formation of phenols-bridged inter-HBs reduces the inter-chain cooperativity/constraints of polyacrylates (as manifested by smaller coupling factor n and dynamic fragility m), which is accompanied by a reduction in α, β_{JG} separation in most hybrids. Interestingly, despite of the effectively reducing inter-chain cooperativity/constraints, a suppressed β_{JG}-peak with amplified α, β_{JG} separation was recognized by increasing the bulkiness of hindered phenols. The anomalous dynamics that the α, β_{JG} separation amplifies with reducing n, can be rationalized by assumption that the crossover time t_c in the Coupling Model might not be a universal quantity and that it could decrease with increasing $\Delta\upsilon_i$.

Electronic Supplementary Information

Electronic supplementary information (ESI) is available free of charge in the online version of this article at http://doi.org/10.1007/s10118-021-2595-y.

ACKNOWLEDGMENTS

This study was financially supported by the National Natural Science Foundation of China (Nos. 51873063 and 51373053).

REFERENCES

1 Ribelles, J. G.; Duenas, J. M.; Pradas, M. M. Dielectric relaxations in poly(methyl acrylate), poly(ethyl acrylate), and poly(butyl

acrylate). *J. Appl. Polym. Sci.* **1989**, *38*, 1145–1157.

2 Shi, G.; Liu, Y.; Wu, G. β_{fast} Relaxation governs the damping stability of acrylic polymer/hindered phenol hybrids. *Macromolecules* **2020**, *53*, 4692–4703.

3 Johari, G. P.; Goldstein, M. Viscous liquids and the glass transition. II. Secondary relaxations in glasses of rigid molecules. *J. Chem. Phys.* **1970**, *53*, 2372–2388.

4 Johari, G. P.; Goldstein, M. Viscous liquids and the glass transition. III. Secondary relaxations in aliphatic alcohols and other nonrigid molecules. *J. Chem. Phys.* **1971**, *55*, 4245–4252.

5 Molinero, V.; Goddard III, W. A. Microscopic mechanism of water diffusion in glucose glasses. *Phys. Rev. Lett.* **2005**, *95*, 045701.

6 Guo, J. H. A theoretical and experimental study of additive effects of physical aging and antiplasticization on the water permeability of polymer film coatings. *J. Pharm. Sci.* **1994,** *83*, 447-449.

7 Burgess, S. K.; Lee, J. S.; Mubarak, C. R.; Kriegel, R. M.; Koros, W. J. Caffeine antiplasticization of amorphous poly(ethylene terephthalate): effects on gas transport, thermal, and mechanical properties. *Polymer* **2015,** *65*, 34-44.

8 Light, R. R.; Seymour, R. W. Effect of sub-T_g relaxations on the gas transport properties of polyesters. *Polym. Eng. Sci.* **1982,** *22*, 857-864.

9 Priestley, R. D.; Rittigstein, P.; Broadbelt, L. J.; Fukao, K.; Torkelson, J. M. Evidence for the molecular-scale origin of the suppression of physical ageing in confined polymer: fluorescence and dielectric spectroscopy studies of polymer-silica nanocomposites. *J. Phys.: Condens. Matter* **2007**, *19*, 205120.

10 Shamblin, S. L.; Tang, X.; Chang, L.; Hancock, B. C.; Pikal, M. J. Characterization of the time scales of molecular motion in pharmaceutically important glasses. *J. Phys. Chem. B* **1999**, *103*, 4113–4121.

11 Johari, G.; Kim, S.; Shanker, R. M. Dielectric relaxation and crystallization of ultraviscous melt and glassy states of aspirin, ibuprofen, progesterone, and quinidine. *J. Pharm. Sci.* **2007**, *96*, 1159–1175.

12 Vyazovkin, S.; Dranca, I. Physical stability and relaxation of amorphous indomethacin. *J. Phys. Chem. B* **2005**, *109*, 18637–18644.

13 Yu, H.; Wang, W.; Bai, H.; Wu, Y.; Chen, M. Relating activation of shear transformation zones to β relaxations in metallic glasses. *Phys. Rev. B* **2010**, *81*, 220201.

14 Wang, Q.; Zhang, S.; Yang, Y.; Dong, Y.; Liu, C.; Lu, J. Unusual fast secondary relaxation in metallic glass. *Nat. Commun.* **2015,** *6*, 1-6.

15 Zhao, Z.; Wen, P.; Wang, W.; Shek, C. Observation of secondary relaxation in a fragile $Pd_{40}Ni_{10}Cu_{30}P_{20}$ bulk metallic glass. *Appl. Phys. Lett.* **2006**, *89*, 071920.

16 Yu, H.; Samwer, K.; Wang, W.; Bai, H. Chemical influence on β-relaxations and the formation of molecule-like metallic glasses. *Nat. Commun.* **2013**, *4*, 2204.

17 Zhao, Z.; Wen, P.; Shek, C.; Wang, W. Measurements of slow β-relaxations in metallic glasses and supercooled liquids. *Phys. Rev. B* **2007**, *75*, 174201.

18 Yu, H.; Samwer, K.; Wu, Y.; Wang, W. Correlation between β relaxation and self-diffusion of the smallest constituting atoms in metallic glasses. *Phys. Rev. Lett.* **2012**, *109*, 095508.

19 Zhu, Z.; Li, Y.; Wang, Z.; Gao, X.; Wen, P.; Bai, H.; Ngai, K. L.; Wang, W. Compositional origin of unusual β-relaxation properties in La-Ni-Al metallic glasses. *J. Chem. Phys.* **2014**, *141*, 084506.

20 Stachurski, Z. Micromechanics of stress relaxation in amorphous glassy PMMA. Part I. Molecular model for anelastic behaviour. *Polymer* **2002,** *43*, 7419-7427.

21 Pfister, L.; Stachurski, Z. Micromechanics of stress relaxation in amorphous glassy PMMA part II: application of the RT model. *Polymer* **2002**, *43*, 7409–7417.

22 Wind, M.; Graf, R.; Renker, S.; Spiess, H. W. Structural reasons for restricted backbone motion in poly (*n*-alkyl methacrylates): degree of polymerization, tacticity and side-chain length. *Macromol. Chem. Phys.* **2005,** *206*, 142-156.

23 Shahin Thayyil, M.; Ngai, K. L.; Prevosto, D.; Capaccioli, S. Revealing the rich dynamics of glass-forming systems by modification of composition and change of thermodynamic conditions. *J. Non-Cryst. Solids* **2015,** *407*, 98-105.

24 de Deus, J. F.; Souza, G. P.; Corradini, W. A.; Atvars, T. D.; Akcelrud, L. Relaxations of poly(methyl methacrylate) probed by covalently attached anthryl groups. *Macromolecules* **2004**, *37*, 6938–6944.

25 Talhavini, M.; Atvars, T. D. Z.; Schurr, O.; Weiss, R. G. Translocation of fluorescent probes upon stretching low-density polyethylene films. Comparison between 'free' and covalently-attached anthryl groups. *Polymer* **1998**, *39*, 3221–3232.

26 Casalini, R.; Snow, A.; Roland, C. Temperature dependence of the Johari–Goldstein relaxation in poly(methyl methacrylate) and poly(thiomethyl methacrylate). *Macromolecules* **2012,** *46*, 330-334.

27 Casalini, R.; Roland, C. Effect of crosslinking on the secondary relaxation in polyvinylethylene. *J. Polym. Sci., Part B: Polym. Phys.* **2010,** *48*, 582-587.

28 Redondo-Foj, B.; Sanchis, M. J.; Ortiz-Serna, P.; Carsí, M.; García, J. M.; García, F. C. The effect of cross-linking on the molecular dynamics of the segmental and β Johari-Goldstein processes in polyvinylpyrrolidone-based copolymers. *Soft Matter* **2015**, *11*, 7171–7180.

29 Redondo-Foj, B.; Carsi, M.; Ortiz-Serna, P.; Sanchis, M.; Vallejos, S.; García, F.; García, J. Effect of the dipole-dipole interactions in the molecular dynamics of poly(vinylpyrrolidone)-based copolymers. *Macromolecules* **2014**, *47*, 5334–5346.

30 Kahle, S.; Korus, J.; Hempel, E.; Unger, R.; Höring, S.; Schröter, K.; Donth, E. Glass-Transition Cooperativity Onset in a Series of Random copolymers poly(*n*-butyl methacrylate-stat-styrene). *Macromolecules* **1997**, *30*, 7214–7223.

31 Lorthioir, C.; Alegria, A.; Colmenero, J. Out of equilibrium dynamics of poly(vinyl methyl ether) segments in miscible poly(styrene)-poly(vinyl methyl ether) blends. *Phys. Rev. E* **2003**, *68*, 031805.

32 Bedrov, D.; Smith, G. D. A molecular dynamics simulation study of relaxation processes in the dynamical fast component of miscible polymer blends. *Macromolecules* **2005**, *38*, 10314–10319.

33 Blochowicz, T.; Rössler, E. Beta relaxation versus high frequency wing in the dielectric spectra of a binary molecular glass former. *Phys. Rev. Lett.* **2004**, *92*, 225701.

34 Ngai, K. L. *Relaxation and diffusion in complex systems*. Springer New York: **2011**, p.232–247.

35 Capaccioli, S.; Paluch, M.; Prevosto, D.; Wang, L.; Ngai, K. L. Many-body nature of relaxation processes in glass-forming systems. *J. Phys. Chem. Lett.* **2012**, *3*, 735-743.

36 Ngai, K. L. Coupling model explanation of salient dynamic properties of glass-forming substances. *IEEE T. Dielect. El. In.* **2001,** *8*, 329-344.

37 Ngai, K. L.; Rendell, R. W. Cooperative dynamics in relaxation: a coupling model perspective. *J. Mol. Liq.* **1993,** *56*, 199-214.

38 Alvarez, F.; Alegra, A.; Colmenero, J. Relationship between the time-domain Kohlrausch-Williams-Watts and frequency-domain Havriliak-Negami relaxation functions. *Phys. Rev. B* **1991**, *44*, 7306–7312.

39 Ngai, K. L.; Gopalakrishnan, T. R.; Beiner, M. Relaxation in poly(alkyl methacrylate)s: Change of intermolecular coupling with molecular structure, tacticity, molecular weight, copolymerization, crosslinking, and nanoconfinement. *Polymer* **2006**, *47*, 7222–7230.

40 Roland, C.; Ngai, K. L. Constraint dynamics and chemical

https://doi.org/10.1007/s10118-021-2595-y

structure. *J. Non-Cryst. Solids* **1994**, *172*, 868-875.

41 Pan, D.; Sun, Z. Influence of chain stiffness on the dynamical heterogeneity and fragility of polymer melts. *J. Chem. Phys.* **2018**, *149*, 234904.

42 Shinyashiki, N.; Spanoudaki, A.; Yamamoto, W.; Nambu, E.; Yoneda, K.; Kyritsis, A.; Pissis, P.; Kita, R.; Yagihara, S. Segmental relaxation of hydrophilic poly(vinylpyrrolidone) in chloroform studied by broadband dielectric spectroscopy. *Macromolecules* **2011**, *44*, 2140–2148.

43 Alegria, A.; Colmenero, J.; Ngai, K. L.; Roland, C. Observation of the component dynamics in a miscible polymer blend by dielectric and mechanical spectroscopies. *Macromolecules* **1994**, *27*, 4486–4492.

44 Meier, G.; Vlassopoulos, D.; Fytas, G. Phase Separation and Glass Transition Intervention in a Polymer Blend. *EPL* **1995,** *30*, 325-330.

45 Park, H.; Bradley, P.; Greisen, P.; Liu, Y.; Mulligan, V. K.; Kim, D. E.; Baker, D.; DiMaio, F. Simultaneous optimization of biomolecular energy functions on features from small molecules and macromolecules. *J. Chem. Theory Comput.* **2016**, *12*, 6201–6212.

46 Cui, W.; Li, J.; Decher, G. Self-Assembled Smart Nanocarriers for Targeted Drug Delivery. *Adv. Mater.* **2016**, *28*, 1302–1311.

47 Cordier, P.; Tournilhac, F.; Soulié-Ziakovic, C.; Leibler, L. Self-healing and thermoreversible rubber from supramolecular assembly. *Nature* **2008,** *451*, 977-980.

48 Weis, P.; Wu, S. Light-switchable azobenzene-containing macromolecules: from UV to near infrared. *Macromol. Rapid Commun.* **2018**, *39*, 1700220.

49 Kuang, X.; Zhou, Y.; Shi, Q.; Wang, T.; Qi, H. J. Recycling of epoxy thermoset and composites *via* good solvent assisted and small molecules participated exchange reactions. *ACS Sustain. Chem. Eng.* **2018**, *6*, 9189–9197.

50 Lin, Y.; Xu, C.; Guan, A.; Wu, G. Tailoring the temperature-dependent viscoelastic behavior of acrylic copolymers by introducing hydrogen bonding interactions. *Polymer* **2019,** *161*, 190–196.

51 Shi, G.; Yin, X.; Wu, G. Thermodynamic phase analysis of acrylic polymer/hindered phenol hybrids: effects of hydrogen bonding strength. *Polymer* **2018,** *153*, 317–324.

52 Yin, X.; Liu, C.; Lin, Y.; Guan, A.; Wu, G. Influence of hydrogen bonding interaction on the damping properties of poly(*n*-butyl methacrylate)/small molecule hybrids. *J. Appl. Polym. Sci.* **2015**, *132*, 41954.

53 Painter, P. C.; Graf, J. F.; Coleman, M. M. Effect of hydrogen bonding on the enthalpy of mixing and the composition dependence of the glass transition temperature in polymer blends. *Macromolecules* **1991**, *24*, 5630–5638.

54 Liu, C.; Yin, X.; Lin, Y.; Guan, A.; Wu, G. Small molecule-mediated glass transition of acrylic copolymers: effect of hydrogen bonding strength on glass transition temperature. *J. Polym. Sci., Part B: Polym. Phys.* **2015,** *53*, 400-408.

55 Zhang, S. H.; Jin, X.; Painter, P. C.; Runt, J. Dynamic homogeneity in mixtures of poly(vinyl methyl ether) with low molecular weight phenolic molecules. *Macromolecules* **2003**, *36*, 7179–7188.

56 Liu, Y.; Shi, G.; Wu, G. Hydrogen bonding-induced anomalous dynamics of polyacrylates mixed with small molecules. *Polymer* **2020**, *201*, 122627.

57 Liu, C.; Liu, Z.; Yin, X.; Wu, G. Tuning the dynamic fragility of acrylic polymers by small molecules: the interplay of hydrogen bonding strength. *Macromolecules* **2015**, *48*, 4196–4206.

58 Masser, K. A.; Runt, J. Dynamics of polymer blends of a strongly interassociating homopolymer with poly(vinyl methyl ether) and poly(2-vinylpyridine). *Macromolecules* **2010**, *43*, 6414–6421.

59 Zhang, S.; Painter, P. C.; Runt, J. Coupling of component segmental relaxations in a polymer blend containing intermolecular hydrogen bonds. *Macromolecules* **2002**, *35*, 9403–9413.

60 Carsi, M.; Sanchis, M.; Diaz-Calleja, R.; Riande, E.; Nugent, M. Effect of cross-linking on the molecular motions and nanodomains segregation in polymethacrylates containing aliphatic alcohol ether residues. *Macromolecules* **2012**, *45*, 3571–3580.

61 Havriliak, S.; Negami, S. A complex plane analysis of α-dispersions in some polymer systems. *J. Polym. Sci., Part C: Polym. Symp.* **1966,** *14*, 99-117.

62 Zhang, S.; Runt, J. Segmental dynamics and ionic conduction in poly(vinyl methyl ether)−lithium perchlorate complexes. *J. Phys. Chem. B* **2004**, *108*, 6295–6302.

63 Bergman, R.; Alvarez, F.; Alegrıa, A.; Colmenero, J. Dielectric relaxation in PMMA revisited. *J. Non-Cryst. Solids* **1998,** *235*, 580-583.

64 Bergman, R.; Alvarez, F.; Alegrıa, A.; Colmenero, J. The merging of the dielectric α- and β-relaxations in poly(methyl methacrylate). *J. Chem. Phys.* **1998**, *109*, 7546–7555.

65 Shuster, M.; Narkis, M.; Siegmann, A. Polymeric antiplasticization of polycarbonate with polycaprolactone. *Polym. Eng. Sci.* **1994**, *34*, 1613–1618.

66 Stukalin, E. B.; Douglas, J. F.; Freed, K. F. Plasticization and antiplasticization of polymer melts diluted by low molar mass species. *J. Chem. Phys.* **2010**, *132*, 084504.

67 Cicerone, M. T.; Douglas, J. F. β-Relaxation governs protein stability in sugar-glass matrices. *Soft Matter* **2012**, *8*, 2983–2991.

68 Schröter, K.; Unger, R.; Reissig, S.; Garwe, F.; Kahle, S.; Beiner, M.; Donth, E. Dielectric spectroscopy in the $\alpha\beta$ splitting region of glass transition in poly(ethyl methacrylate) and poly(*n*-butyl methacrylate): different evaluation methods and experimental conditions. *Macromolecules* **1998**, *31*, 8966–8972.

69 Garwe, F.; Schonhals, A.; Beiner, M.; Schroter, K.; Donth, E. Molecular cooperativity against locality at glass transition onset in poly(*n*-butyl methacrylate). *J. Phys.: Condens. Matter* **1994**, *6*, 6941–6945.

70 Angell, C. A. Formation of glasses from liquids and biopolymers. *Science* **1995,** *267*, 1924-1935.

71 Ngai, K. L.; Capaccioli, S. Relation between the activation energy of the Johari-Goldstein β relaxation and T_g of glass formers. *Phys. Rev. E* **2004**, *69*, 031501.

72 Ngai, K. L. *Relaxation and diffusion in complex systems*. Springer: New York. **2011**, p.63–73.

73 Afandak, A.; Eslami, H. Ion-pairing and electrical conductivity in the ionic liquid 1-*n*-butyl-3-methylimidazolium methylsulfate [Bmim][MeSO$_4$]: molecular dynamics Simulation study. *J. Phys. Chem. B* **2017**, *121*, 7699–7708.